Magnetic response of local moments in disordered metals

1995 J. Phys.: Condens. Matter 7 6853

(http://iopscience.iop.org/0953-8984/7/34/010)

J. Phys.: Condens. Matter 7 (1995) 6853–6868. Printed in the UK

Magnetic response of local moments in disordered metals

David G Rowan, Yolande H Szczech, Michael A Tusch and David E Logan

Physical and Theoretical Chemistry Laboratory, Oxford University, South Parks Road, Oxford OX1 3QZ, UK

Received 16 May 1995

Abstract. We study the magnetic response properties of both site and spatially disordered Anderson–Hubbard models via a random-phase-type approximation for collective excitations about stable, inhomogeneous mean-field ground states. For the site-disordered model, zero-temperature transitions between paramagnetic, disordered antiferromagnetic and spin-glass-like ground states are examined. Within broken symmetry phases, a microscopic picture of the response of the inhomogeneous distribution of local magnetic moments to an external field is obtained, and the role of disorder in leading to a strong site differential enhancement in local susceptibilities is highlighted.

1. Introduction

The interplay between disorder and electron interactions, in governing electronic and magnetic properties of disordered solids, is a fundamental problem in condensed matter theory to which a rich variety of theoretical approaches has been developed over the last decade or more; see e.g. [1, 2] and references therein. Central to this endeavour is an understanding of the role of local magnetic moments occurring in disordered metals with delocalized charge carriers, each arising from the same 'set' of electrons.

Among the simplest models with which to investigate these matters are one-band Anderson–Hubbard models (AHM), specified by the Hamiltonian

$$H = \sum_{i,\sigma} \epsilon_i n_{i\sigma} - \sum_{i,j,\sigma}{}' t_{ij} c^{\dagger}_{i\sigma} c_{j\sigma} + U \sum_i n_{i+} n_{i-} \tag{1.1}$$

(in standard notation), with interactions embodied in the on-site Hubbard U. The quenched disorder may enter either via (a) site disorder [3–9] in the distribution of site energies $\{\epsilon_i\}$ or (b) spatial disorder [10–12] in the site centres of mass, leading to off-diagonal disorder in the one-electron transfer matrix elements $\{t_{ij}\}$. Both types of AHM (at half filling) will be considered in this paper, with an emphasis on the former.

The general strategy we adopt is in principle straightforward, and twofold. First, for a given disorder realization at any chosen point in the disorder–interaction plane, to treat disorder exactly (via numerical study) and ascertain mean-field 'saddle point' solutions at the level of spin-rotationally invariant, fully unrestricted Hartree–Fock (UHF), and second, to examine the response properties of, and collective excitations about, the broken symmetry disordered mean-field states via a random phase approximation (RPA) in its general form; this enables, via loop expansions, subsequent study of the feedback of quantum spin fluctuations. Such an approach is natural in many respects, and has proven very successful for the half-filled pure Hubbard model on the $d = 2$ dimensional square lattice, even (and

0953-8984/95/346853+16$19.50

particularly) in the strong-coupling regime; see e.g. [13, 14]. A central point is of course the stability of the broken symmetry mean-field state: only if this is properly stable against particle–hole excitations will fluctuations about it, treated at RPA level, be bounded [15]; and a necessary condition for such is the use of spin-rotationally invariant UHF.

In a previous paper [8] we have studied, at UHF level alone, a site-disordered AHM on a $d = 3$ simple cubic lattice, with nearest-neighbour hopping matrix elements $t_{ij} = t$, and with the site energies regarded as independent random variables drawn from a common Gaussian distribution, $g(\epsilon)$, of variance Δ^2. The model is specified simply by (i) the scaled interaction strength $\tilde{U} = U/B$ with $B = 12t$ the electronic bandwidth of the unperturbed ($U = 0 = \Delta$) simple cubic lattice, and (ii) $\tilde{\Delta} = \Delta/B$, a scaled measure of the site disorder. At half filling, magnetic and electric phases in the $(\tilde{\Delta}, \tilde{U})$ plane were deduced by direct sampling of a range of possible broken symmetry UHF states. Particular emphasis was given to site differential resolution of a wide range of physical properties, which is central in developing a microscopic picture of the interplay between disorder and interactions; even at mean-field level this leads, for example, to a suggestion of two-fluid-like segregation of charge carriers and local magnetic moments.

In the present paper we study the corresponding magnetic response properties of the disordered local moment phases, at RPA level. Linear response properties of the mean-field states, and the generalized RPA susceptibility matrix, are outlined and discussed formally in section 2. In section 3 we analyse both the phase boundary to local moment formation and the disordered antiferromagnet/spin glass transition via an RPA stability analysis. We turn to the inhomogeneous magnetic response of the system in section 4, as reflected in the distribution of local magnetic susceptibilities, and focus on the evolution with disorder (at constant $\tilde{U}$) as it is increased through the metal towards a metal–(gapless) insulator transition. Disorder, in producing a range of local environments, leads naturally to local moment formation on an inhomogeneous scale. In addition, however, while the mean-field local moments themselves vary only little as disorder is increased, a strong disorder-induced enhancement of the local susceptibilities for moment carrying sites is found. This has significant implications for observable Knight shifts and the bulk magnetic susceptibility. To ensure the findings are not specific to the site-disordered AHM, we discuss briefly a corresponding study of the spatially disordered model directly applicable to e.g. doped semiconductors.

2. UHF+RPA

For any given disorder realization, the fully unrestricted Hartree–Fock (UHF) Hamiltonian corresponding to a generic AHM is given by

$$H^0 = \sum_{i,\sigma} \epsilon_i n_{i\sigma} - \sum_{i,j,\sigma}{}' t_{ij} c^\dagger_{i\sigma} c_{j\sigma} + U \sum_i \{\tfrac{1}{2}\bar{n}_i n_i - 2\bar{\boldsymbol{S}}_i \cdot \boldsymbol{S}_i\} \tag{2.1}$$

where $n_i = \sum_\sigma n_{i\sigma}$ is the local charge operator, $\boldsymbol{S}_i$ is the (vector) spin operator for site i, and the overbars denote an expectation value over the $T = 0$ UHF ground state. The UHF state is of course a single determinant, formed by occupying the UHF single-particle states $\{|\Psi_\alpha\rangle\}$ up to the Fermi level, F. Quasiparticle states are expanded in terms of the local site spin-orbitals $\{|\phi_{i\sigma}\rangle\}$, namely $|\Psi_\alpha\rangle = \sum_{i,\sigma} a_{i\alpha\sigma}|\phi_{i\sigma}\rangle$; and note that the $|\Psi_\alpha\rangle$ are *not* constrained to be pure spin-orbitals (as is necessary to guarantee spin-rotational invariance). Since $H^0 \equiv H^0(\{\bar{n}_i, \bar{\boldsymbol{S}}_i\})$, a self-consistent solution is naturally required: $H^0|\Psi_\alpha\rangle = E_\alpha|\Psi_\alpha\rangle$,

together with the self-consistency equations

$$\bar{S}_{i\mu} = \sum_{\alpha<F} A^{\dagger}_{i\alpha}\sigma^{\mu}A_{i\alpha} \tag{2.2a}$$

$$\bar{n}_i = \sum_{\sigma}\bar{n}_{i\sigma} = \sum_{\sigma}\left(\sum_{\alpha<F}|a_{i\alpha\sigma}|^2\right) \tag{2.2b}$$

where $A_{i\alpha}$ is the column vector

$$A_{i\alpha} = \begin{pmatrix} a_{i\alpha\uparrow} \\ a_{i\alpha\downarrow} \end{pmatrix} \tag{2.2c}$$

and σ^{μ} ($\mu = x, y, z$) are the Pauli matrices.

These equations specify the most general, spin-rotationally invariant, form of UHF. We refer to this as 'Heisenberg spin' UHF meaning that, in a broken symmetry local moment regime, the possibility of non-collinear mean-field spin configurations is permitted. Self-consistent broken symmetry UHF *solutions* obtained thereby may, however, be purely Ising-like with fully collinear mean-field spins/local moments. This occurs for the site-disordered model at half filling, and throughout the disorder–interaction plane ($\tilde{\Delta}, \tilde{U}$) [8]. The simplifications arising in this case will be discussed in section 2.2; for the present we consider the general case of Heisenberg-like mean-field solutions.

2.1. Linear response

Collective excitations about the UHF state may be obtained by considering directly the linear response of any UHF state to the application, at time $t = 0$, of an arbitrary space- and time-dependent external magnetic field, $\{^{ex}h_i(t)\}$, via the Zeeman coupling $H_z = g\sum_i S_i \cdot {}^{ex}h_i(t)$, with $g = 2$ the electronic g-factor. For $t > 0$, the expectation values entering equation (2.1) naturally acquire a time dependence, expressed by

$$\bar{S}_i(t) = \bar{S}_i + \delta\bar{S}_i(t) \qquad \bar{n}_i(t) = \bar{n}_i + \delta\bar{n}_i(t). \tag{2.3}$$

The Hamiltonian may then be written as

$$H(t) = H^0 + H^f(t) \tag{2.4}$$

with H^0 the unperturbed UHF Hamiltonian (2.1). $H^f(t)$ carries all the t dependence and is given by

$$H^f(t) = g\sum_i S_i \cdot h_i(t) + \tfrac{1}{2}U\sum_i n_i\delta\bar{n}_i(t). \tag{2.5}$$

Here, $h_i(t)$ is the *total* magnetic field at site i, consisting of the external plus an induced (internal) field,

$$h_i(t) = {}^{ex}h_i(t) + {}^{int}h_i(t) \tag{2.6}$$

where ${}^{int}h_i(t) = -U\delta\bar{S}_i(t)$.

The response of the UHF state to the applied field is characterized by the time evolution of $\delta\bar{S}_{i\mu}(t)$ and $\delta\bar{n}_i(t)$; and we seek the linear response of the system to the total field. From standard linear response theory [16], this is given by

$$\delta\bar{O}(t) = -\mathrm{i}\int_0^t \mathrm{d}t' \,\langle 0|[O_H(t), H^f_H(t')]|0\rangle \tag{2.7}$$

where $|0\rangle$ denotes the unperturbed UHF state, and $O_H(t) = e^{iH^0 t} O e^{-iH^0 t}$. Evaluation of equation (2.7) yields, after lengthy algebra, the frequency (ω) dependence of the field-induced local magnetic moments and charges, namely

$$F^\mu(\omega) = \sum_\nu {}^0\chi^{\mu\nu}(\omega) M^\nu(\omega). \tag{2.8}$$

$F(\omega)$ is a $4N$-component vector (with N the number of sites) with elements

$$F_i^\mu(\omega) = \begin{cases} -\delta\bar{S}_{i\mu}(\omega) & \mu \in \{x, y, z\} \\ \dfrac{1}{2}\delta\bar{n}_i(\omega) & \mu = c \end{cases} \tag{2.9}$$

including both spin and charge (c) components. Likewise $M(\omega)$, which acts as a generalized total field, has elements

$$M_i^\mu(\omega) = \begin{cases} h_{i\mu}(\omega) = {}^{ex}h_{i\mu}(\omega) - U\delta\bar{S}_{i\mu}(\omega) & \mu \in \{x, y, z\} \\ -\dfrac{1}{2}U\delta\bar{n}_i(\omega) & \mu = c. \end{cases} \tag{2.10}$$

The $4N \times 4N$ matrix ${}^0\chi(\omega)$, with elements ${}^0\chi_{ij}^{\mu\nu}(\omega)$, is the UHF susceptibility matrix, including in general spin–spin, charge–charge and spin–charge response functions. With the operator $O_{i\mu}$ defined by

$$O_{i\mu} = \begin{cases} -S_{i\mu} & \mu \in \{x, y, z\} \\ \dfrac{1}{2}n_i & \mu = c \end{cases} \tag{2.11a}$$

according to whether spin or charge components are considered, ${}^0\chi_{ij}^{\mu\nu}(\omega)$ is given by

$${}^0\chi_{ij}^{\mu\nu}(\omega) = 2i\int_{-\infty}^{\infty} e^{i\omega t}\theta(t)\langle 0|[O_{i\mu}(t), O_{j\nu}]|0\rangle. \tag{2.11b}$$

This is readily evaluated in terms of the eigenvalues and eigenvectors of the UHF H^0, equation (2.1), and yields

$${}^0\chi_{ij}^{\mu\nu}(\omega) = 2\sum_{\alpha,\beta} \frac{(\bar{n}_\beta - \bar{n}_\alpha)}{(E_\alpha - E_\beta) + \omega + i\eta} (A_{i\alpha}^\dagger \sigma^\mu A_{i\beta})(A_{j\beta}^\dagger \sigma^\nu A_{j\alpha}) \tag{2.12}$$

where $\eta = 0+$, $\bar{n}_\alpha = \theta(E_F - E_\alpha)$ is the occupation number of single-particle state α in the UHF state, and for $\mu = c$ we define $\sigma^c_{\sigma_1\sigma_2} = -\frac{1}{2}\delta_{\sigma_1\sigma_2}$.

Equation (2.8) describes the dynamic response of the UHF state to the total field. Of direct physical relevance, however, is the response to the externally applied magnetic field. This follows directly from equations (2.8,10):

$$F^\mu(\omega) = \sum_\nu \chi^{\mu\nu}(\omega)\, {}^{ex}h^\nu(\omega) \tag{2.13}$$

with the $4N \times 4N$ Hermitian susceptibility matrix $\chi(\omega)$ given by

$$\chi(\omega) = [1 - U\,{}^0\chi(\omega)Q]^{-1}\,{}^0\chi(\omega) \tag{2.14}$$

where Q is diagonal, with $Q_{ij}^{\mu\nu} = \delta_{\mu\nu}\delta_{ij}$ for $\mu \in \{x, y, z\}$ and $Q_{ij}^{\mu\nu} = -\delta_{\mu\nu}\delta_{ij}$ for $\mu = c$. Equation (2.14) may also be obtained diagrammatically by consideration of the analogous time-ordered particle–hole Green functions, within the random phase approximation (RPA) [16]. The linear response of any UHF state to an arbitrary external magnetic field is thus given exactly by the RPA susceptibility.

Equations (2.12) and (2.14) are the basic RPA equations. From (2.12), knowledge of the UHF state alone (the $\{E_\alpha\}$ and $\{a_{i\alpha\sigma}\}$) enables a determination of ${}^0\chi(\omega)$ for any

ω. $\chi(\omega)$ then follows from (2.14), which is also practically convenient since, with $\{\lambda_\gamma\}$ and $\{V_\gamma\}$ denoting respectively the eigenvalues and eigenvectors of the matrix product ${}^0\chi'(\omega) = {}^0\chi(\omega)Q$, Eq. (2.14) reduces to

$$\chi_{ij}^{\mu\nu}(\omega) = \{\delta_{\nu x} + \delta_{\nu y} + \delta_{\nu z} - \delta_{\nu c}\} \sum_\gamma V_{i\gamma}^\mu \frac{\lambda_\gamma}{1 - U\lambda_\gamma} (V_{i\gamma}^\nu)^*. \tag{2.15}$$

Thus, for given ω, diagonalization of the $4N$-dimensional ${}^0\chi'(\omega)$ is sufficient to determine the RPA $\chi(\omega)$, hence circumventing explicit solution of the conventional RPA eigenvalue problem of dimension $O(N^2)$, and in consequence permitting study of much larger system sizes (N) if, as with disorder present, the problem must of necessity be solved at a finite-size level. Collective excitations occur at frequencies corresponding to the poles of $\chi(\omega)$, i.e. from (2.15) at ω values such that $1 - U\lambda_\gamma(\omega) = 0$, which may thus be found pointwise [17].

Most importantly, the mean-field (UHF) state is stable against particle–hole excitations—and thus a true minimum on the Hartree–Fock 'surface'—provided the poles of $\chi(\omega)$ occur solely on the real ω-axis, or equivalently provided the static $\chi(0)$ has no negative eigenvalues, i.e. from (2.15) provided $\lambda_\gamma \leqslant U^{-1}$ for all $\lambda_\gamma(\omega = 0)$. In a broken spin symmetry regime there will of course be zero-energy Goldstone modes ($\max \lambda_\gamma(0) = U^{-1}$) corresponding to global spin rotations of the mean-field spins: three such for a Heisenberg spin UHF solution (with non-collinear local moments); and two Goldstone modes for an Ising spin solution with fully collinear local moments.

2.2. Ising-like mean-field states

The UHF+RPA equations above are general, and possibly deceptively simple. With a Heisenberg spin UHF solution, for example, spin and charge excitations are inherently coupled, with no partitioning of the susceptibility tensor $\chi^{\mu\nu}(\omega)$. However, the problem simplifies somewhat for an Ising-like UHF solution with wholly collinear local moments lying in the z-direction.

First, the self-consistent UHF single-particle states are pure spin-orbitals, $|\Psi_{\alpha\sigma}\rangle = \sum_i a_{i\alpha\sigma}|\phi_{i\sigma}\rangle$; and H^0 (equation (2.1)) becomes spin separable, $H^0 = \sum_\sigma H_\sigma^0$, with H_σ^0 (such that $H_\sigma^0|\Psi_{\alpha\sigma}\rangle = E_{\alpha\sigma}|\Psi_{\alpha\sigma}\rangle$) given by

$$H_\sigma^0 = \sum_i \epsilon_{i\sigma} n_{i\sigma} - \sum_{i,j}{}' t_{ij} c_{i\sigma}^\dagger c_{j\sigma}. \tag{2.16a}$$

Here $\epsilon_{i\sigma}$, the effective σ spin site energy for site i, is given by

$$\epsilon_{i\sigma} = \epsilon_i + U\bar{n}_{i-\sigma} = \epsilon_i + \tfrac{1}{2}U[\bar{n}_i - \sigma\mu_i] \tag{2.16b}$$

in terms of the local charge $\bar{n}_i$ (as in (2.2b)) and the sole (z-) component of the local magnetic moment,

$$\mu_i \equiv 2\bar{S}_{iz} = \bar{n}_{i\uparrow} - \bar{n}_{i\downarrow}. \tag{2.17}$$

Secondly, transverse spin excitations decouple from longitudinal spin and charge excitations, the resultant RPA $\chi^{\mu\nu}(\omega)$ partitioning into two disjoint $2N \times 2N$ sectors. The lowest-lying excitations about the UHF state occur in the transverse spin sector, $\chi^{\mu\nu}(\omega)$ with $\mu \in \{x, y\}$, on which we focus. Further, with a trivial transformation from local magnetic fields h_{jx}/h_{jy} to $h_{j\pm} = h_{jx} \pm ih_{jy}$, the transverse susceptibility itself separates into two disjoint $N \times N$ blocks, $\chi^{-+}(\omega)$ and $\chi^{+-}(\omega)$, each of which (for $\omega = 0$) contain a single

Goldstone mode provided the UHF state is particle–hole stable. The resultant $\chi^{-+}(\omega)$ is given simply by the more familiar RPA form

$$\chi^{-+}(\omega) = [1 - U\,{}^0\chi^{-+}(\omega)]^{-1}\,{}^0\chi^{-+}(\omega) \tag{2.18}$$

with the corresponding UHF ${}^0\chi^{-+}(\omega)$ given by

$${}^0\chi_{ij}^{-+}(\omega) = \mathrm{i}\int_{-\infty}^{\infty} \mathrm{d}t\ \mathrm{e}^{\mathrm{i}\omega t}\theta(t)\langle 0|[S_{i-}(t), S_{j+}]|0\rangle \tag{2.19a}$$

and thus by

$${}^0\chi_{ij}^{-+}(\omega) = \sum_{\alpha>F>\beta}\left\{\frac{a_{i\alpha\uparrow}a_{j\alpha\uparrow}a_{i\beta\downarrow}a_{j\beta\downarrow}}{(E_{\alpha\uparrow} - E_{\beta\downarrow}) - \omega - \mathrm{i}\eta} + \frac{a_{i\alpha\downarrow}a_{j\alpha\downarrow}a_{i\beta\uparrow}a_{j\beta\uparrow}}{(E_{\alpha\downarrow} - E_{\beta\uparrow}) + \omega + \mathrm{i}\eta}\right\} \tag{2.19b}$$

in terms of the eigenvalues $\{E_{\alpha\sigma}\}$ and (pure real) eigenvector coefficients $\{a_{i\alpha\sigma}\}$ of the Ising spin Hamiltonian, equation (2.16*a*).

Finally, excepting the ω-poles of ${}^0\chi^{-+}(\omega)$ (which do not coincide with those of $\chi^{-+}(\omega)$), ${}^0\chi^{-+}(\omega)$ is a real, symmetric $N \times N$ matrix; and for any such ω may thus be diagonalized by an orthogonal matrix v such that ${}^0\chi^{-+}(\omega)v_\gamma = \lambda_\gamma v_\gamma$. From (2.18) the RPA $\chi^{-+}(\omega)$ is also diagonalized by v_γ, with eigenvalues $\lambda_\gamma/(1 - U\lambda_\gamma)$, whence

$$\chi_{ij}^{-+}(\omega) = \sum_\gamma v_{i\gamma}\frac{\lambda_\gamma}{1 - U\lambda_\gamma}v_{j\gamma} \tag{2.20}$$

is the Ising-like analogue of equation (2.15).

3. Magnetic phases

Self-consistent UHF was used recently [8] to find locally stable, inhomogeneous mean-field ground states for the $\frac{1}{2}$-filled Gaussian site-disordered model on a simple cubic lattice. For any disorder realization at a chosen point in the $(\tilde{\Delta}, \tilde{U})$-plane, the mean-field ground state was determined on energetic grounds. The bulk magnetic character of UHF solutions is determined by magnetic ordering of the local moments $\mu_i \equiv 2\bar{S}_{iz}$, reflected in the relative phases of the $\{\mu_i\}$ as characterized by the spin density [7]

$$S_z(k) = N^{-1}\sum_i \mu_i \exp(\mathrm{i}k \cdot R_i). \tag{3.1}$$

For all $(\tilde{\Delta}, \tilde{U})$ studied, the local moment phases were found to be Ising-like, with $S_z^{\mathrm{tot}} = S_z(0) = 0$; and three distinct magnetic phases occur [8]: disordered paramagnetic (P), antiferromagnetic (AF) and spin-glass-like (SG) phases. In the non-interacting limit $\tilde{U} = 0$, the ground state is trivially paramagnetic ($\mu_i = 0$ for all sites i). For all $\tilde{U} > 0$, in the $\tilde{\Delta} = 0$ pure Hubbard limit, and because the simple cubic lattice is bipartite, the UHF ground state is a pure two-sublattice Néel AF [18], with $|S_z(k)| = \delta_{k,\pi}|\mu|$ where $|\mu| \equiv |\mu_i|$ is the sublattice moment magnitude. Within the $(\tilde{\Delta}, \tilde{U})$-plane, at sufficiently large $\tilde{U}$ the UHF ground state is a disordered AF: $|S_z(k)|$ is clearly dominated by a strong $k = \pi$ peak, with magnitude somewhat less than but on the order of the mean moment magnitude per site, $|\mu| = N^{-1}\sum_i |\mu_i|$. For smaller interaction strengths an SG phase results: $|S_z(k)|$ shows small peaks at numerous k-vectors, with none dominant and no hint of long-ranged order, and the P phase is found to persist at sufficiently weak interaction strengths. The resultant UHF phase diagram in the $(\tilde{\Delta}, \tilde{U})$-plane (for $N = 512$ sites [8]) is shown as part of figure 1. Metallic/insulating phase boundaries are also indicated, consisting of metallic (M), gapless insulating (I) and gapped Hubbard insulating (HI) phases; full details are given in [8].

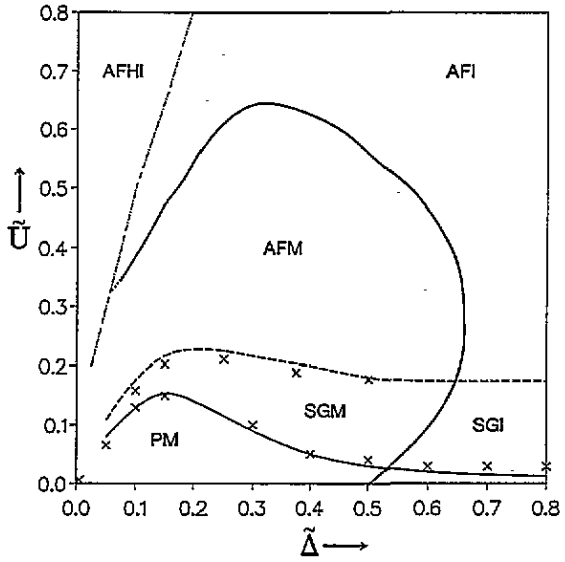

Figure 1. Mean field phases in the disorder-interaction plane, $(\tilde{\Delta}, \tilde{U})$. AF: antiferromagnet; SG: spin glass; P: paramagnet; M: metal; I: insulator; HI: Mott–Hubbard insulator. Crosses show the phase boundary to local moment formation, and the AF–SG transition boundary, deduced from the present study.

The magnetic phase boundaries of [8] were obtained simply by direct sampling of a wide range of possible self-consistent UHF states. No attempt was made to study directly transitions between different phases, and the results were not always unambiguous: for example, it was not clear whether a direct AF–SG transition occurs. Here, we thus consider first the magnetic phase boundaries via a stability analysis at RPA level, beginning with the phase boundary to local moment formation coming from the paramagnetic regime.

3.1. Local moment formation

The paramagnetic (P) phase is confined to weak interaction strengths (figure 1), but its occurrence over a non-vanishing $\tilde{U}$ interval for $\tilde{\Delta} = 0$ accords with the expectation that disorder, in removing the Fermi surface nesting characteristic of the unperturbed $(\tilde{U} = 0 = \tilde{\Delta})$ lattice, will lead to a P regime for sufficiently low $\tilde{U}$, analogous to the $\frac{1}{2}$-filled pure Hubbard model on non-bipartite cubic lattices [19]. The HF solutions here are of the restricted type, and the phase boundary to local moment formation is obtained readily using equations (2.18,20) for $\chi^{-+}(\omega = 0)$ (henceforth denoted χ). Namely, for any given disorder realization at a chosen $\tilde{\Delta}$, increase $\tilde{U}$ from the non-interacting limit and find the critical interaction strength $\tilde{U}_c(\tilde{\Delta})$ for which the largest eigenvalue, $\max(\lambda_\gamma)$, of ${}^0\chi$ becomes equal to $1/U$, signalling an instability of the paramagnetic (restricted) mean-field solution to a broken symmetry local moment phase. Then (and only then) examine the variation of $\tilde{U}_c(\tilde{\Delta})$ with different disorder realizations at the chosen $\tilde{\Delta}$.

The results of this are indicated by crosses on the phase diagram, figure 1; and the variation of $\tilde{U}_c(\tilde{\Delta})$ with disorder realizations is small, within $\sim \pm 0.02$ of the mean for all $\tilde{\Delta}$. Full agreement with the UHF phase boundary is clearly found (in all cases within error bars). Further, Fourier resolution of the Goldstone eigenvector $\{v_{i\gamma}\}$ at the instability point shows essentially uniform contributions from most k-values, i.e. the transition is to a SG

phase, again in agreement with the mean-field results. In fact, this occurs for disorders as low as $\tilde{\Delta} = 0.005$, suggesting that for all $\tilde{\Delta} > 0$ an SG moment phase is first accessed.

The above procedure contrasts with a common approximation (see e.g. [5]) in which, instead of sampling individual disorder realizations, an attempt is made to infer the phase boundary to local moment formation via an approximate calculation of the disorder-averaged susceptibility matrix $\bar{\chi}$. Disorder averaging restores translational invariance, and if equation (2.18) is iterated in powers of ${}^0\chi$, and all fluctuation moments $\overline{({}^0\chi - {}^0\bar{\chi})^m}$ neglected, then Fourier transformation of the resultant $\bar{\chi}$ yields the algebraic expression $\bar{\chi}(k) = {}^0\bar{\chi}(k)/(1 - U\,{}^0\bar{\chi}(k))$. This $\bar{\chi}(k)$ must diverge at a single k-vector—for any disorder $\tilde{\Delta}$. In fact, it predicts [5] that the local moment phase first accessed with increasing $\tilde{U}$ is always an AF, $k = \pi$, with the critical $\tilde{U}_c(\tilde{\Delta})$ *increasing* with increasing disorder. This is strongly at variance with the correct result, pointing to the importance of disorder-induced fluctuations in ${}^0\chi$ and the inapplicability of a generalized Stoner criterion.

3.2. *AF and SG phases*

Local moment formation, and hence the P–SG boundary, is thus accessible via the restricted HF states appropriate to the P phase (which we note appear to be the sole UHF solutions in the paramagnet [8]). However, equations (2.18–20) apply equally to the magnetic phases provided the underlying broken symmetry UHF states are stable, i.e. provided $\lambda_\gamma < U^{-1}$ for all modes γ other than the characteristic Goldstone mode, $\max(\lambda_\gamma) = U^{-1}$. An RPA stability analysis may thus also be applied to the AF–SG phase boundary in figure 1.

To this end we note another helpful limit of the $\frac{1}{2}$-filled site-disordered model. Namely, for any finite disorder, $\tilde{\Delta}$, and in the strong-coupling limit $\tilde{U} \to \infty$ (in practice $\tilde{U} \gg \tilde{\Delta}$), the model reduces to the *non-disordered* pure AF Heisenberg model. Thus, for any disorder realization at a chosen value of $\tilde{\Delta}$, the disorder is effectively 'switched on' as $\tilde{U}$ is decreased from strong coupling. This enables properties of the self-consistent mean-field states to be tracked continuously in $\tilde{U}$ through the disordered AF and towards the SG phase, with the mean-field ground state recalculated self-consistently at each successive $\tilde{U}$ point.

To illustrate this, figure 2 shows $S_z(k = \pi)$ against $\tilde{U}$ for a single disorder realization

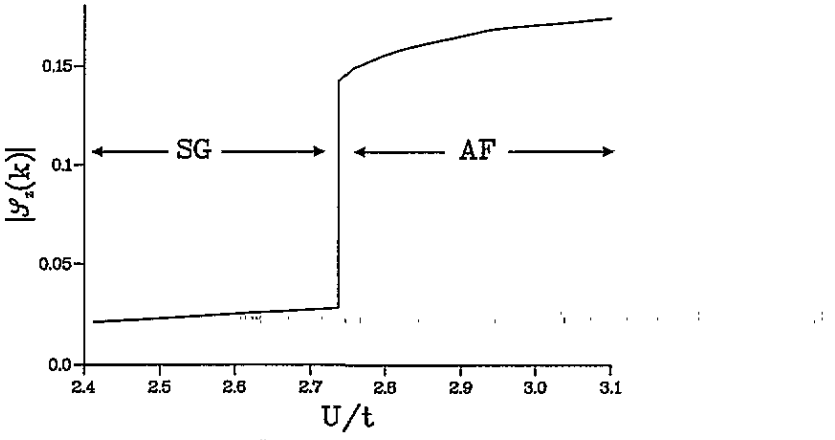

Figure 2. $S_z(\pi)$ against $\tilde{U}$ for a single disorder realization at $\tilde{\Delta} = 0.25$, showing the antiferromagnet/spin glass transition.

at $\tilde{\Delta} = 0.25$ (and for $N = 216$ sites). $\mathcal{S}_z(\boldsymbol{k})$ is defined by

$$\mathcal{S}_z(\boldsymbol{k}) = |S_z(\boldsymbol{k})| \Big/ \sum_{\boldsymbol{k}} |S_z(\boldsymbol{k})| \tag{3.2}$$

with $S_z(\boldsymbol{k})$ as in equation (3.1). $\mathcal{S}_z(\pi)$ may be regarded essentially as the AF order parameter, and for the pure two-sublattice Néel AF occurring at $\tilde{\Delta} = 0$, $\mathcal{S}_z(\boldsymbol{k}) = \delta_{\boldsymbol{k},\pi}$. As $\tilde{U}$ is decreased through the AF phase, $\mathcal{S}_z(\pi)$ decreases continuously. That the state is indeed AF is confirmed from the full $\boldsymbol{k}$ dependence of $\mathcal{S}_z(\boldsymbol{k})$, which is dominated by $\boldsymbol{k} = \pi$ as described earlier; and the fact that $\mathcal{S}_z(\pi) < 1$ simply reflects that the AF, while exhibiting long-ranged order, is increasingly 'dirty' due to the disorder, see also [8]. At a critical interaction strength, $\tilde{U}_c = 0.228$, the AF state becomes unstable and changes to a SG phase; $\mathcal{S}_z(\pi)$ correspondingly undergoes a discontinuous change at $\tilde{U}_c$ to a smaller value characteristic of the SG (whose scaling with system size, N, we examine below).

In tandem with this behaviour, the largest eigenvalue $\lambda_{\max} = \max(\lambda_\gamma)$ of the static UHF susceptibility matrix ${}^0\chi$ (see (2.20)) is precisely $1/U$ in either broken symmetry phase; this reflects both the presence of the characteristic Goldstone mode—corresponding to a global spin rotation which preserves the relative phases of the mean-field spins—and the particle–hole stability of the mean-field states. Note that while the AF Goldstone mode leads throughout the AF phase to the expected divergence in the ($\omega = 0$) staggered susceptibility $\chi(\boldsymbol{k} = \pi)$, in neither phase alone do the Goldstone modes contribute to the corresponding uniform susceptibility $\chi(\boldsymbol{k} = \boldsymbol{0})$, since the spatial Fourier transform of the Goldstone eigenvector $\{v_{iy}\}$ is readily shown to be proportional to $S_z(\boldsymbol{k})$, and $S_z^{\text{tot}} \equiv S_z(\boldsymbol{0}) = 0$ for all Ising-like UHF solutions. However, as $\tilde{U}$ approaches from either phase the transition point at $\tilde{U}_c$, a *second* mode λ_v tends to $1/U_c$ from below, signalling the AF↔SG transition evident in figure 2 (and enabling thereby an accurate determination of the critical $\tilde{U}_c$).

At the first-order transition point there are thus in effect three soft modes: one Goldstone mode for the AF ($\tilde{U} = \tilde{U}_c+$), one Goldstone mode for the SG ($\tilde{U} = \tilde{U}_c-$) and a third soft mode which interconnects the AF and SG solutions. The latter leads to a divergence in the uniform $\chi(\boldsymbol{0})$ as $\tilde{U} \to \tilde{U}_c$, namely $\chi(\boldsymbol{0}) = A|\tilde{U} - \tilde{U}_c|^{-\mu}$ with an exponent $\mu = 1$ determined from careful numerical analysis. We do not, however, believe that the divergence will itself survive the thermodynamic limit, since the soft-mode eigenvector $\{v_{iv}\}$—which interconnects the AF and SG solutions via a global but non-phase-preserving spin rotation—has weight on at least as many $\boldsymbol{k}$-vectors as contribute to $S_z(\boldsymbol{k})$ for the SG phase; and if (as shown below) $S_z(\boldsymbol{k})$ is of order $O(N^{-1})$ in the SG, we expect the susceptibility divergence to be washed out in the thermodymanic limit.

An AF–SG transition thus indeed appears to occur, and to be first order, and the behaviour described above occurs for each disorder realization at any chosen $\tilde{\Delta}$, although at the finite-size level there is somewhat more variation in $\tilde{U}_c(\tilde{\Delta})$ with disorder realizations than in the P–SG case, up to $\sim \pm 0.04$ from the mean at larger $\tilde{\Delta} \gtrsim 0.5$. With this procedure we find thereby the AF–SG phase boundary indicated by crosses in figure 1, which is in good agreement with that inferred from the indirect approach of [8].

Finally, we comment on the scaling with system size (N) of $\mathcal{S}_z(\boldsymbol{k})$ in the SG phase, noting first that, in an AF regime, $\mathcal{S}_z(\pi)$ (as shown in figure 2) does not show a significant variation with N. As remarked above, however, the SG $\mathcal{S}_z(\boldsymbol{k})$ shows small peaks at numerous $\boldsymbol{k}$-vectors, with none dominant. By way of illustration, figure 3 shows, for $\tilde{\Delta} = 0.25$ and $\tilde{U} = \frac{1}{6}$, a logarithmic plot of the N dependence of the disorder-averaged $\bar{\mathcal{S}}_z(\boldsymbol{k})$ at *each* permitted non-zero $\boldsymbol{k}$-vector, and for $N = 64$, 216, 512 and 10^3 sites. From the straight line with gradient -1 (indicated on the figure) it is clear that $\bar{\mathcal{S}}_z(\boldsymbol{k}) \sim O(N^{-1})$ for all $\boldsymbol{k}$, as indeed expected for a SG phase.

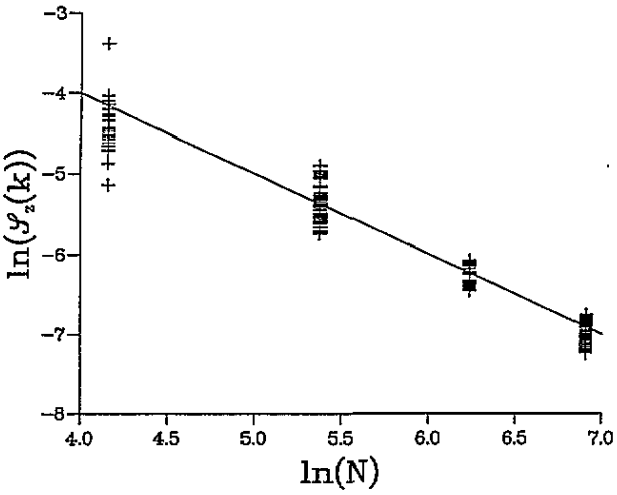

Figure 3. At $(\tilde{\Delta}, \tilde{U}) = (\frac{1}{4}, \frac{1}{6})$ in the SG phase: $\ln \bar{S}_z(k)$ for each non-zero k-vector versus $\ln N$, for $N = 64$, 216, 512 and 10^3 sites. The straight line shown has gradient -1.

4. Inhomogeneous magnetic response

Our aim here is to examine at RPA level the magnetic response of the disordered local moment phases on an inhomogeneous scale, focussing in particular on a site differential resolution of the bulk susceptibility into its local components.

To this end we consider specifically application of a static, uniform field to the system, and (see section 2.1) define components of the uniform static susceptibility via $\chi_u^{\mu\nu} = N^{-1} \sum_{ij} \chi_{ij}^{\mu\nu}$. Due to net charge conservation, $\chi_u^{\mu c} = 0$ (see (2.11)); thus, only the magnetic sector of $\chi_u^{\mu\nu}$ is non-zero. Whether the stable UHF solutions are Ising-like or Heisenberg-like, the presence of Goldstone modes in the magnetic sector implies that, under the applied field, the mean-field spins undergo a global (spin flop) rotation such that the overall response in the field direction is equal to the largest eigenvalue of the matrix $\{\chi_u^{\mu\nu}\}$, thus minimizing the second-order field contribution to the energy, $\Delta E/N = -\frac{1}{2} \sum_{\mu\nu} h_\mu \chi_u^{\mu\nu} h_\nu$ (where h here denotes the applied field). For the particular case of Ising-like mean-field states, appropriate to the site-disordered model, $\chi_u^{\mu\nu}$ is diagonal with components χ_u^{-+}, χ_u^{+-} and χ_u^{zz}. Throughout most of the phase plane, $\chi_u^{-+} \gg \chi_u^{zz}$, whence the spin–flop transition is such that the Ising spin-axis lies perpendicular to the applied field. Thus, only the transverse static susceptibility $\chi_u^{-+} = \chi_u^{+-} \equiv \chi_u$ is probed; and on this we focus.

Electron interactions, in leading to local moment formation, and disorder in producing a range of local site environments, naturally result together in a spatially inhomogeneous distribution of local mean-field magnetization and charge. As mentioned above, this is true even in the predominant AF phase: although the $\{\mu_i\}$ are 'phase locked' to produce net AF order, the moment carrying sites are distributed randomly in space, and disorder leads to a strong site differential distribution of local moment *magnitudes*. As discussed in [8], the site moment magnitude $|\mu_i|$ is governed largely by the bare site energy ϵ, which may be considered in effect as a 'window' on its local environment, and sites with bare site energies $|\epsilon_i| \lesssim \frac{1}{2}U = E_F$ are found to carry the strongest moments, while those outside this range carry progressively weaker moments, being predominantly doubly occupied by electrons

($\epsilon_i \lesssim -\frac{1}{2}U$) or empty ($\epsilon_i \gtrsim \frac{1}{2}U$). Accordingly [8], the inhomogeneous distribution of local magnetization is generally well characterized by $|\mu(\epsilon)| = N_\epsilon^{-1} \sum_{i:\epsilon_i=\epsilon} |\mu_i|$, the mean moment magnitude per site of given site energy ϵ (with N_ϵ the number of such sites, given via $N_\epsilon/N = g(\epsilon)\,\mathrm{d}\epsilon$). We seek now to study the analogous site differential resolution of χ_u.

4.1. Site-disordered model

To probe the inhomogeneous magnetic response of the system, and relate it to the mean-field local moment distribution $|\mu(\epsilon)|$, note that the bulk static χ_u may be written as $\chi_u = N^{-1} \sum_i \chi_i$, where χ_i ($\equiv \chi_i^{-+}$) given by $\chi_i = \sum_j \chi_{ij}$ is the local RPA susceptibility of site i, and we deconvolute χ_u as

$$\chi_u = \int \chi(\epsilon) g(\epsilon)\,\mathrm{d}\epsilon \tag{4.1}$$

where, for any disorder realization at the chosen disorder $\tilde{\Delta}$,

$$\chi(\epsilon) = N_\epsilon^{-1} \sum_{i:\epsilon_i=\epsilon} \chi_i \tag{4.2}$$

is the mean local susceptibility per site of given site energy ϵ. $\chi(\epsilon)$ thus embodies the inhomogeneous response of the disordered local moment distribution, itself reflected in $|\mu(\epsilon)|$. To illustrate the effect of disorder on $\chi(\epsilon)$, we consider a fixed interaction strength $\tilde{U} = \frac{1}{2}$, with increasing disorder $\tilde{\Delta} = \frac{1}{8}, \frac{1}{4}, \frac{1}{2}$. Figure 4 shows $\chi(\epsilon)$ and $|\mu(\epsilon)|$ against $\tilde{\epsilon} = \epsilon/B$ for $\tilde{\Delta} = \frac{1}{8}$ (a), $\frac{1}{4}$ (b)and $\frac{1}{2}$ (c), averaged over a number of typical disorder realizations for $N = 216$ sites. To relate this parameter range to that of the metal–(gapless) insulator transition (MIT), figure 1 shows that at $\tilde{\Delta} = \frac{1}{8}$ the system is a gapless insulator, while by $\tilde{\Delta} = \frac{1}{4}$ the system is well within the metallic regime, and as $\tilde{\Delta}$ is increased further an MIT at $\tilde{\Delta} \simeq 0.56$ is approached.

At low disorder, $\tilde{\Delta} = \frac{1}{8}$, the system's response is rather uniform: the vast majority of sites carry strong local moments, and $\chi(\epsilon)$ for such is close to the $\tilde{\Delta} = 0$ pure Hubbard limit of $0.39/t$ (where $\chi_i \equiv \chi_u$ for all sites i, whence $\chi(\epsilon = 0) \equiv \chi_u = 0.39/t$). In addition, $\chi(\epsilon)$ is only slightly enhanced over the local Pauli susceptibilities appropriate to the non-interacting but disordered limit, where $\chi(\epsilon) = D(\epsilon; E_F)$, the local density of Fermi level states also shown in figure 4. However, as clearly shown by figure 4, increasing disorder leads to a strong, site differential enhancement in the local susceptibilities. The enhancement is greatest for $|\tilde{\epsilon}| \lesssim \frac{1}{2}\tilde{U}$—i.e. the strong-local-moment sites—and occurs even though the mean-field local moment profile $|\mu(\epsilon)|$ itself varies little with disorder. This is already evident by $\tilde{\Delta} = \frac{1}{4}$ in the metal (figure 4b) but it increases markedly with disorder until (figure 4c) by $\tilde{\Delta} = \frac{1}{2}$—close to the MIT—$\chi(\epsilon)$ for the strong-local-moment sites is more than an order of magnitude larger than either that for the $\tilde{\Delta} = 0$ or $\tilde{U} = 0$ limits; and is similarly in excess of the 'Pauli-like' $\chi(\epsilon)$ values typical of non-moment sites with $|\tilde{\epsilon}| \gtrsim \frac{1}{2}\tilde{U}$.

This behaviour has a ready physical explanation. That $\chi(\epsilon)$ is largest on strong-local-moment sites reflects appreciable overlap of low-ω collective transverse spin excitations on these sites, as is evident from the Lehmann representation of $\chi_i(\omega)$. Direct analysis [20] of the low-ω poles of $\chi(\omega)$ shows these to be spin-wave-like for the $(\tilde{\Delta}, \tilde{U})$ values in question, and hence naturally associated with the strong-moment carrying sites, and the disorder-induced enhancement in $\chi(\epsilon)$ thus reflects a progressive softening of the low-ω transverse spin spectrum with increasing disorder.

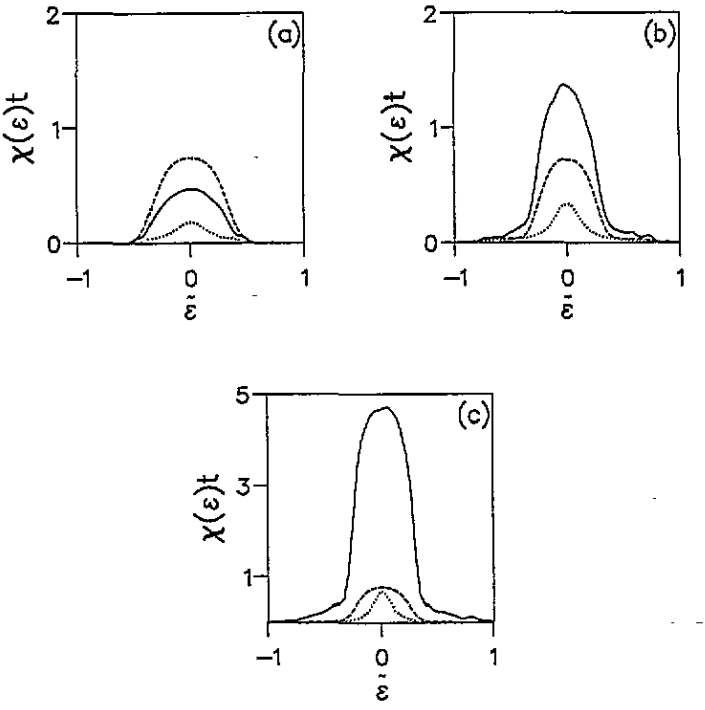

Figure 4. Distribution of local susceptibilities $\chi(\epsilon)$ against $\tilde{\epsilon} = \epsilon/B$ (solid lines), for $\tilde{U} = \frac{1}{2}$ and $\tilde{\Delta} = \frac{1}{8}$ (a) $\frac{1}{4}$ (b) and $\frac{1}{2}$ (c). Also shown are the corresponding local moment distributions $|\mu(\epsilon)|$ (dashed lines) and the non-interacting $\tilde{U} = 0$ Pauli local susceptibilities (dotted lines). Note the change of vertical scale in (c).

What effect is the above behaviour likely to have on observable properties of disordered, interacting systems? Consider two complementary probes of the magnetism. The total uniform spin susceptibility, probed for example by ESR methods, is simply the sum of all individual, local susceptibilities; see (4.1). In the present case, as $\tilde{\Delta}$ is increased towards the MIT, the bulk χ_u increases, since the marked enhancement in $\chi(\epsilon)$ for strong-moment sites more than compensates for the diminishing fraction of such sites. (Recall that while the mean local moment magnitude *per site* of given ϵ, $|\mu(\epsilon)|$, varies little with $\tilde{\Delta}$, the overall fraction of strong-moment sites $\sim 2\int_0^{U/2} g(\epsilon)\,d\epsilon$, and thus decreases progressively as the disorder is increased.) A complementary probe of local magnetism is the Knight shift in an NMR experiment, the local Knight shift under the electron–nuclear contact interaction, K_i, being proportional to the local site susceptibility, χ_i. Clearly, therefore, inhomogeneity in the local susceptibilities $\{\chi_i\}$—as reflected in $\chi(\epsilon)$—will lead to a distribution of local Knight shifts, with sites carrying the strongest local moments experiencing the largest signal displacement. In practice, however, an NMR spectrometer has a finite field range, outside which resonances are not detected; this range is typical of Pauli-like susceptibilities. The findings above thus imply that, as disorder is progressively increased in the metallic regime, the very sites which dominate the observed bulk susceptibility χ_u may be completely projected out of the detected Knight shift signal, which will thus by contrast be dominated by the Pauli-like $\chi(\epsilon)$ of sites outside the local moment range.

This behaviour is qualitatively close to that observed by Alloul and Dellouve [21] for low-temperature Si:P, as the phosphorus number density ρ is decreased progressively

in the metallic regime, towards and through the MIT occurring at a critical density $\rho_c \simeq 3.8 \times 10^{18}\text{cm}^{-3}$. The measured bulk spin susceptibility is progressively and strongly paramagnetically enhanced over the non-interacting Pauli value (the enhancement beginning at $\rho \sim 2\rho_c$). By contrast, a steadily diminishing fraction of spins is picked up in the average detected ^{31}P Knight shift $\langle K \rangle$, which falls off rapidly but continuously as the MIT is approached and crossed. The authors themselves ascribe this behaviour to the 'projecting out' of an increasing fraction of P sites—intuitively, those carrying strong local moments—as ρ is decreased towards and through ρ_c. The site-disordered Anderson–Hubbard model is not of course directly applicable to Si:P, which is well caricatured by a spatially disordered AHM [10]. To ensure the findings above are not specific to the site-disordered case, we have therefore carried out a preliminary study of the spatially disordered system, on which we now briefly report.

4.2. Spatially disordered model

The Hamiltonian for the spatially disordered system is:

$$H = -\sum_{\substack{i,j \\ \sigma}}{}' t_{ij} c^{\dagger}_{i\sigma} c_{j\sigma} + U \sum_i n_{i+} n_{i-}. \tag{4.3}$$

Here the quenched disorder occurs in the distribution of hopping matrix elements, $t_{ij} = t(R_{ij})$ with $R_{ij} = |\boldsymbol{R}_i - \boldsymbol{R}_j|$, arising from spatial disorder in the site ('P') centres of mass $\{\boldsymbol{R}_i\}$. t_{ij} is taken to be of the form

$$t_{ij} = t_0(1 + R_{ij}/a_H)\exp(-R_{ij}/a_H) \tag{4.4}$$

with a_H the effective Bohr radius; specification of any $\{\boldsymbol{R}_i\}$ prescribes a particular realization of the $\{t_{ij}\}$. The model is again characterized by two parameters: the scaled interaction strength U/t_0, and the reduced density measure $a^*_H = \rho^{\frac{1}{3}} a_H$. The band is again half filled.

The model is treated essentially as before. For illustration we choose $U/t_0 = 5/8$ (a reasonable choice for Si:P), and study a density regime spanning the MIT. A previous HF study [10] of the model has shown clearly the instability of the disordered Fermi liquid to local moment formation, via analysis of restricted HF states; but since these non-magnetic solutions are found to be unstable for all densities studied, consideration of broken symmetry UHF is a necessary prerequisite to the study of the magnetic response of the disordered local moment phase.

In the $\tilde{U} = 0$ non-interacting limit the critical value of a^*_H for the Anderson MIT is known to be [22] $a^*_c = 0.22$. From study of the inverse participation ratio for systems of several hundred sites, similar to those used [8] for the site-disordered model—and eschewing the question of particle–hole stability of the broken symmetry UHF states, to which mean-field properties such as e.g. the ipr and distribution of local moment magnitudes are found to be insensitive (see [8])—we estimate $a^*_c \simeq 0.28$ for $U/t_0 = 5/8$; the precise value is not however central to the following analysis.

To study the magnetic response, it is of course imperative that the UHF solutions are particle–hole stable. These are almost invariably Heisenberg-like, with non-collinear local moments whose magnitudes we continue to denote by $|\mu_i|$ $(= (\sum_\alpha \bar{S}^2_{i\alpha})^{\frac{1}{2}})$. Figure 5 shows the resultant probability density $P(|\mu|) = N^{-1} \sum_i \delta(|\mu_i| - |\mu|)$ for a wide density range spanning the MIT. From this it is clear, as expected physically for the spatially disordered system (and in contrast to the site-disordered model), that with increasing disorder—decreasing density—an increasing fraction of sites carry strong local moments. For example, the fraction of sites with $|\mu_i| > 0.5$ is ~16% at $a^* = 0.35$ and ~25% at $a^* = 0.3$ (rising to

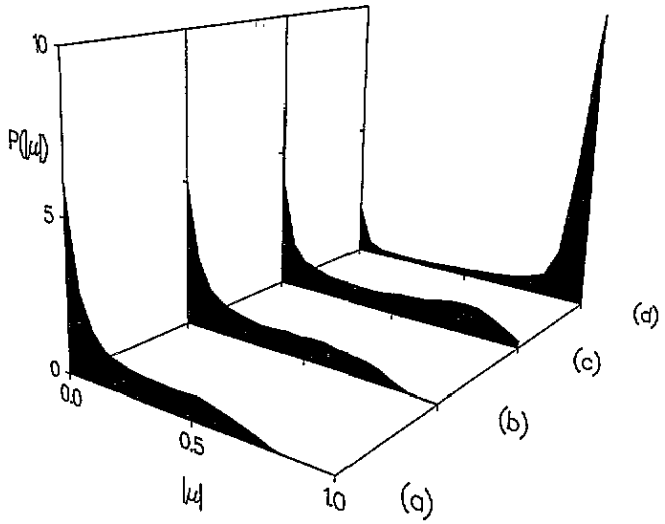

Figure 5. Probability density of local moment magnitudes for the spatially disordered model, $P(|\mu|)$ against $|\mu|$. For $U/t_0 = \frac{5}{8}$ and $a^* = \rho^{\frac{1}{3}} a_H = 0.35$ (a), 0.30 (b), 0.25 (c) and 0.15 (d).

~45% at $a^* = 0.25$ in the insulator); for $|\mu_i| > 0.75$, the corresponding figures are ~1% and 6% (and ~20%).

Due to the slow convergence rate of the iterative self-consistency procedure for UHF solutions which are Heisenberg-like, and the need to sample many disorder realizations at any chosen a^*, system sizes of only $N = 50$ sites were employed; this is small, but sufficient to make the principal point. With the resultant mean-field solutions, the total uniform static susceptibility may be calculated, accounting carefully for the spin flop transition as described at the beginning of section 4. The total uniform static susceptibility is again given by $\chi_u = N^{-1} \sum_i \chi_i$, where the corresponding local susceptibility $\chi_i = \sum_j [m^T \chi m]_{ij}$ with m the eigenvector corresponding to the largest eigenvalue of $\{\chi_u^{\mu\nu}\}$.

For the site-disordered model, local susceptibilities were studied via $\chi(\epsilon)$, the mean local susceptibility per site of given site-energy ϵ. In the spatially disordered problem there is no such easy measure of 'local environment', but one does expect intuitively that the larger the local moment of a site, the greater will be its typical local magnetic response. In analogy to equations (4.1,2) we thus deconvolute χ_u as

$$\chi_u = \int_0^1 \chi(|\mu|) P(|\mu|)\, \mathrm{d}|\mu| \tag{4.5}$$

where, for any disorder realization at the chosen a^*,

$$\chi(|\mu|) = N_{|\mu|}^{-1} \sum_{i:|\mu_i|=|\mu|} \chi_i \tag{4.6}$$

is the mean local susceptibility *per site* of given local moment magnitude $|\mu|$, and $N_{|\mu|}$ (such that $N_{|\mu|}/N = P(|\mu|)\, \mathrm{d}|\mu|$) is the number of such sites. The $|\mu|$ dependence of $\chi(|\mu|)$ thus reflects the inhomogeneous magnetic response of the disordered local moment distribution, itself embodied in $P(|\mu|)$.

Figure 6 shows the resultant $\chi(|\mu|)$ against $|\mu|$ for $a^* = 0.35$ and 0.30. The system is metallic in either case, the former corresponding to a density of around twice that for the MIT, the latter to about 25% in excess of ρ_c. As with the site-disordered model, strong site

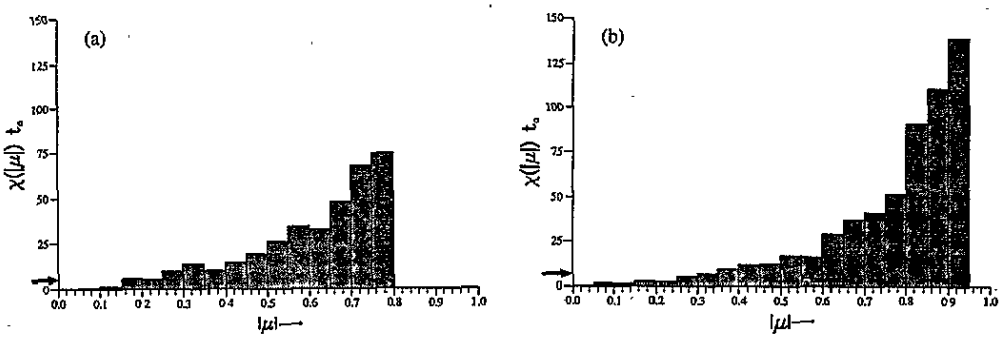

Figure 6. Local susceptibilities $\chi(|\mu|)$ against $|\mu|$ for the spatially disordered model, for $a^* = 0.35$ (a) and 0.30 (b), both in the metallic regime. The Pauli susceptibility for the corresponding non-interacting electron gas at the same a^* is marked on the vertical axis.

differential enhancement of the local susceptibilities is again evident: $\chi(|\mu|)$ for the strong-local-moment sites is well over an order of magnitude larger than the Pauli susceptibility for the corresponding non-interacting electron gas at the same a^*, as marked on the vertical axis; and is even more largely in excess of $\chi(|\mu|)$ values typical of the statistically predominant low-$|\mu|$ sites (although we note in passing that $\chi(|\mu|)$ for these sites will be underestimated, since for any finite-size system in the non-interacting or restricted HF limits, the zero-frequency χ_l values calculated directly via equations (2.12,14) are strictly zero, see also [5]).

In the spatially disordered case too, therefore, strong site differential magnetism is evident, resulting in a strongly inhomogeneous distribution of local Knight shifts. With decreasing density, an increasing fraction of the strong-local-moment sites will clearly be projected out of the detected Knight shift signal, and will also contribute to the progressive enhancement of the total χ_u.

In contrast to the site-disordered model, however, there is a further important consideration in the spatially disordered system. It has been argued [11] that low-temperature thermodynamics in the metallic phase—focusing in particular on the magnetic susceptibility—is dominated by localized spin excitations in very rare spatial regions. The basic idea [11] is that at any mean number density ρ, rare statistical density fluctuations lead to a non-vanishing probability of producing an isolated spin in a region of radius $r \gg \rho^{-\frac{1}{3}}$, which is sufficiently isolated from the rest of the system that its exchange coupling to conduction electrons is exponentially small; and that the resultant local moments remain unquenched (by the Kondo effect in particular) down to the lowest temperatures, whence such rare sites dominate the bulk susceptibility at low T. Support for this view comes also from recent work [23] on a spatially disordered single-impurity Anderson model.

The present study does not of course consider the Kondo effect (and is for $T = 0$). It is however statistically very unlikely that we produce these rare density fluctuations in the small finite-size calculations above: such quasi-isolated sites would show up as having a local moment $|\mu_i|$ exponentially close to unity, with a massively enhanced χ_l and an extremely low-frequency, localized spin excitation in the corresponding RPA spectrum. Were we to detect them, they would overwhelmingly dominate (and almost certainly overestimate) the bulk χ_u, even though they would constitute but a rather small fraction of sites carrying significant local moments. Although we do not pick up these rarest sites, which will dominate χ_u, we believe it likely that the large enhancement of the local susceptibilities

for the strong-local-moment sites that we *do* observe will be important in determining the fraction of sites which are projected out of the detected Knight shift. Support for this resides in the observation [21] that, for ρ in the vicinity of ρ_c, some 50% or more of ^{31}P nuclei are projected out of the detected Knight shift, with those that are detected being rather insensitive to T; whereas by contrast some 5–10% of local moments dominate bulk thermodynamic properties (see e.g. [23]) in strongly T-dependent terms.

Acknowledgments

It is a pleasure to acknowledge helpful discussions with M Eastwood, T Koslowski, W von Niessen, J Osborne and S Sachdev. We are grateful to the SERC, EPSRC (Condensed Matter Physics) and British Council for financial support.

References

[1] Lee P A and Ramakrishnan T V 1985 *Rev. Mod. Phys.* **57** 287
[2] Belitz D and Kirkpatrick T R 1994 *Rev. Mod. Phys.* **66** 261
[3] Ma M 1982 *Phys. Rev.* B **26** 5097
[4] Shimizu A, Aoki H and Kamimura H 1986 *J. Phys. C: Solid State Phys.* **19** 725
[5] Singh A 1988 *Phys. Rev.* B **37** 430
[6] Zimanyi G T and Abrahams E 1990 *Phys. Rev. Lett.* **64** 2719
[7] Dasgupta C and Halley J W 1993 *Phys. Rev.* B **47** 1126
[8] Tusch M A and Logan D E 1993 *Phys. Rev.* B **48** 14843
[9] Logan D E and Siringo F 1993 *J. Phys.: Condens. Matter* **5** 1841
[10] Milovanović M, Sachdev S and Bhatt R N 1989 *Phys. Rev. Lett.* **63** 82
[11] Bhatt R N and Fisher D S 1992 *Phys. Rev. Lett.* **68** 3072
[12] Bush I J, Logan D E and Madden P A 1994 *Z. Phys. Chem.* **184** 25
[13] Schrieffer J R, Wen Z-G and Zhang S-C 1989 *Phys. Rev.* B **39** 11663
[14] Singh A and Tesanović Z 1990 *Phys. Rev.* B **41** 614, 11457
[15] Thouless D J 1972 *The Quantum Mechanics of Many-Body Systems* (New York: Academic)
[16] Fetter A L and Walecka J D 1971 *Quantum Theory of Many-Particle Systems* (New York: McGraw-Hill)
[17] While a principal part is strictly understood in (2.15) as it stands, the behaviour of $\mathrm{Im}\,\chi(\omega)$ in the vicinity of any pole may be found by straightforward analytical continuation, $\lambda_\gamma \to \lambda_\gamma(\omega + is)$ with $|s| \to 0$ and $\mathrm{sgn}(s)$ appropriately chosen.
[18] Penn D R 1966 *Phys. Rev.* **142** 350
[19] Grensing D, Marsch E and Steeb W-H 1978 *Phys. Rev.* B **17** 2221
Long M W 1991 *The Hubbard Model: Recent Results* ed M Rasetti (London: World Scientific) pp 1–19
[20] Szczech Y H and Logan D E to be published
[21] Alloul H and Dellouve P 1987 *Phys. Rev. Lett.* **59** 578
[22] Root L J, Bauer J D and Skinner J L 1988 *Phys. Rev.* B **37** 5518
Bauer J D, Logovinsky V and Skinner J L 1988 *J. Phys. C: Solid State Phys.* **21** L993
[23] Lakner M, von Löhneysen H, Langenfeld A and Wölfle P 1994 *Phys. Rev.* B **50** 17064